International Journal of Power Electronics and Drive System (IJPEDS)
Vol. 8, No. 3, September 2017, pp. 1109~1116
ISSN: 2088-8694, DOI: 10.11591/ijpeds.v8i3.pp1109-1116

Design and Implementation of BLDC Motor with Integrated Drive Circuit

Joon Sung Park, Ki-Doek Lee
Korea Electronics Technology Intitute, Korea

Article Info

Article history:

Received Mar 28, 2017
Revised Jun 6, 2017
Accepted Jul 3, 2017

Keyword:

Brushless DC (BLDC) motor
Integrated drive circuit
Inverter
Motor drive
Pulse width modulation (PWM)

ABSTRACT

The trend in the motor applications is to reduce weight and volume by increasing the efficiency. Because of the advantage of high efficiency and high density, interest in brushless DC motors and drives is increasing. Unlike DC motors, the brushless DC (BLDC) motors require inverter circuit and position detector. In this paper, we deal with the optimization of the BLDC motor, the inverter, and the position detector. The inverter is optimized to be mounted on the BLDC motor. This paper deals primarily with the design and implementation aspects of the BLDC motor and the integrated drive circuit. Experimental results for the prototype of the BLDC motor with integrated dirve circuit in the laboratory are presented to validate the feasibility.

Corresponding Author:

Ki-Doek Lee,
Intelligent Mechatronics Research Center,
Korea Electronics Technology Institute,
203-201 B/D #388, Songnaedae-ro, Wonmi-gu, Bucheon-si, Gyeonggi-do, Korea, 14502.
Email: kdlee@keti.re.kr

1. INTRODUCTION

Because of the growing interest in global environmental protection and depletion of petroleum resources, there is growing concern in energy efficiency. Under these situations, the mechanical parts in the industry are being replaced by electronic methods. For the driving system, DC motor and brushless dc (BLDC) motor are widely used. DC motor has ever been applied in various industrial applications because their controls and characteristics are simple. In an industrial point of view, DC motor is more used than others at small motor. However, DC motor systems have low efficiency, low reliability, bulky construction, and need of maintenance [1],[2]. Those features are unsuitable for downsizing trend. In recent years, the BLDC motor is receiving more interest for most industrial applications, because of the elimination of the brush and commutator, which reduces audible noise and radio-frequency interference (RFI) problems. Moreover, the BLDC motor has a number of advantages such as high efficiency, high power factor, and low maintenance cost [1]-[5]. The motor efficiency should be increased and the motor size should be made compact. On the basis of the technological growth of power electronics and electric machines, the trend in the industrial applications is to replace conventional DC motor with the BLDC motor. This paper deals primarily with the design and implementation aspects of the BLDC motor and the integrated drive circuit which are consisted with the BLDC motor, the inverter, and the position detector. For the design of the BLDC motor, this study presents analytic approach for the design of the BLDC motor. And the design of the integrated drive system with the position detector is presented. Experimental results for the prototype of the BLDC motor with integrated dirve circuit in the laboratory are presented to validate the feasibility of the proposed integrated BLDC motor system.

2. EQUIVALENT MAGNETIC CIRCUIT MODEL

Generally, when the number of poles is increased, the iron loss and induced torque are also increased in the constant output condition. The pole and slot number affects winding factor and the winding factor is related to torque constant. Therefore, pole/slot ratio should be determined by considering winding factor, manufacturing capabilities, and iron loss [6]. By considering these points, the pole/slot ratio is determined as 12/9. The BLDC motor with 12 pole/9 slot has double layered concentrated winding and high energy permanent magnet in rotor core. The fundamental object of motor design process is to determine the back-emfs of the BLDC motor. Therefore, air gap flux density calculation is required in the first step. In this study, the magnetic circuit model is used to compute design parameters and finite element analysis is applied to confirm the results and execute specific design. Figure 1 shows the magnetic circuit of the BLDC motor. In Figure 2, the magnetic flux Φ can be expressed as

$$\Phi = \frac{2R_m}{2R_m + 2K_r R_g}\Phi_r = \frac{1}{1 + K_r \frac{R_g}{R_m}}\Phi_r \quad (1)$$

where R_m and R_g are magnet and air gap reluctance respectively, Φ_r is flux source, and K_r is reluctance factor which increases air gap reluctance slightly to compensate for the missing steel reluctance [7].

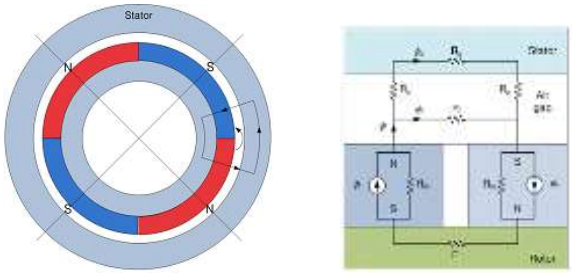

Figure 1. Motor structure and flux path Figure

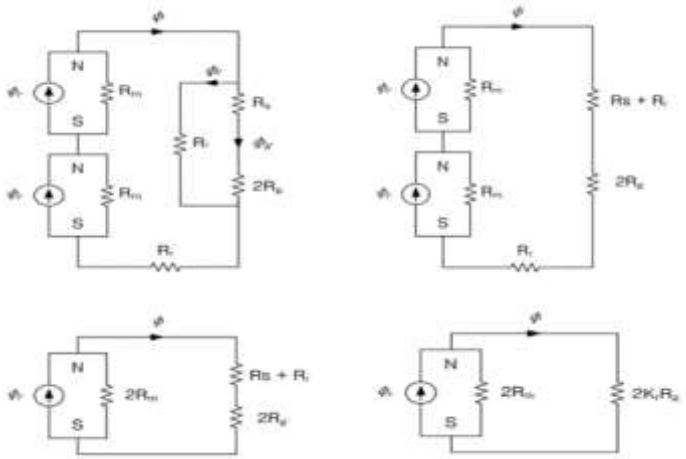

Figure 2. Simplified magnetic circuit

The air gap flux can be written as

$$\Phi_g = K_l \Phi = \frac{K_l}{1 + K_r \frac{\mu_r g A_m}{l_m A_g}}\Phi_r \quad (2)$$

where K_l is the flux leakage factor. Considering the flux linkage waveform which varies from a maximum positive value Φ to a maximum negative value $-\Phi$, back-emf over half an electric cycle is given by

$$E = \frac{d\lambda}{dt} = \omega_e \frac{d\lambda}{d\theta_e} p\omega_m \frac{2N\Phi_g}{\pi a} = K_e \omega_m \quad (3)$$

where λ is flux linkage and p is number of pole pairs, N is the number of conductors per phase, and a is the number of parallel paths. Using the winding coefficient K_w, the back-emf constant K_e can be expressed as

$$K_e = \frac{2pN\Phi_g K_w}{\pi a} \quad (4)$$

The width of teeth body and stator yoke are determined by (5) and (6) [6].

$$w_{tb} = \frac{2\pi R_{ro} B_g}{N_s K_{st} B_t} \quad (5)$$

$$w_{sy} = \frac{\pi R_{ro} B_g}{N_m K_{st} B_{sy}} \quad (6)$$

where R_{ro}, K_{st}, N_s, N_m, B_t, and B_{sy} are rotor radius, stacking factor, number of slot and pole, flux density of teeth and stator yoke, respectively. 2D finite element simulations are used to confirm electromagnetic characteristics of the designed motor. Figure 3 shows magnetic flux density distribution and flux line of the simulated model and Figure 4 shows the back-emf property of designed motor at rotational speed of 1,000 rpm.

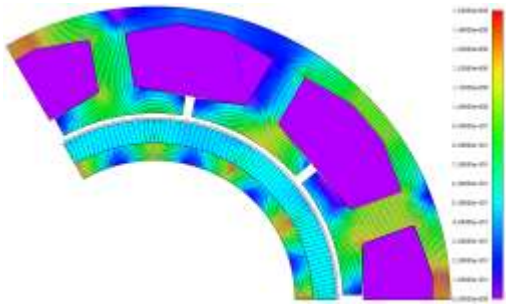

Figure 3. Magnetic flux density distribution and flux line

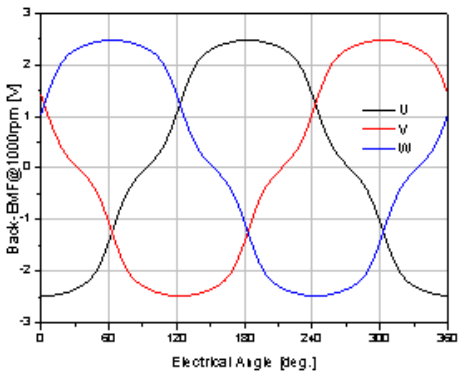

Figure 4. Back-EMFs at 1,000rpm

Figure 5 shows simulated results on the assumption that input voltage of 24 V is applied to the motor. Average torque is about 0.05 Nm and input current is predicted as approximately 1 A at rated condition. From those results, we could estimate EMF or torque constant and no-load speed. By the determined parameters including coil resistance and applied voltage, revolution speed and input current characteristics with respect to loading torque are estimated. As expected, eddy current loss which is proportional to the square of frequency and flux density is dominant at rate condition of 3,400 rpm. The design parameters of the proposed motor are shown in Table 1, finally.

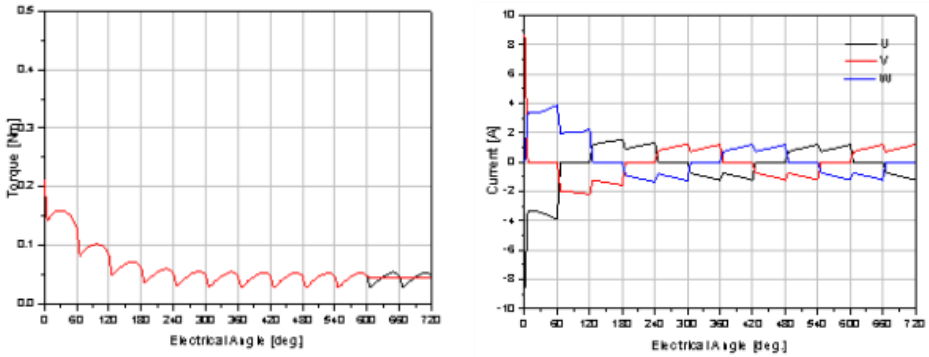

(a) Simulation result of torque (b) Simulation result of phase currents

Figure 5. Back-EMFs at 1,000rpm

Table 1. BLDC motor specifications

Item	Unit	Value
Motor type	-	3Φ,12p/9s
Rated speed	rpm	3,400
Rated power	W	15
Input voltage	V	24
Diameter of stator core	mm	34
Diameter of rotor core	mm	21

3. DESIGN OF INTEGRATED DRIVE

A disadvantage in the DC motors is their brush and commutator requirement. The brushes tend to arc, which generates RFI. The mechanical action of the brush sliding along the commutator can also create audible noise that may be objectionable in some applications. The brushes in some low cost DC motors may also need to be replaced in as little as 1,000h of operation. The commutator and brush assembly can fail in a catastrophic manner under worst-case conditions, such as during a stalled or locked rotor. When electronic controls are added to a brush motor, it is sometimes worth upgrading to a brushless motor for increased performance. A BLDC motor eliminates the commutator and the brush. And the BLDC motor operates indirectly from DC. Unlike the DC motor, there are no mechanical commutation equipment which are the brush and commutator. The BLDC motor is popular for industrial applications that cannot tolerate brushes and in equipment that requires good speed control plus high efficiency [1],[2].

Figure 6 shows the typical inverter configuration and stator equivalent circuit. Generally, a BLDC motor is wound in three-phase Y configuration. This configuration connects end of each phase together to make the motor neutral point. This is then driven by an inverter with 120° commutation method. At any step, only two of the three phases are conducting current where current flows into one phase and then out another. For instance, when phase A and B conduct current, phase C is floating.

A transition from one step to another step is called commutation. So, totally, there are six steps in one electrical cycle. The first step is AB (phase A and B conducting current), then to AC, to BC, to BA, to CA, to CB and then the pattern is repeated. For producing maximum torque, the inverter should be commutated every 60 electrical degrees so that current is in phase with the back-emf. The conducting interval for each phase is 120 electrical degrees, or two steps.

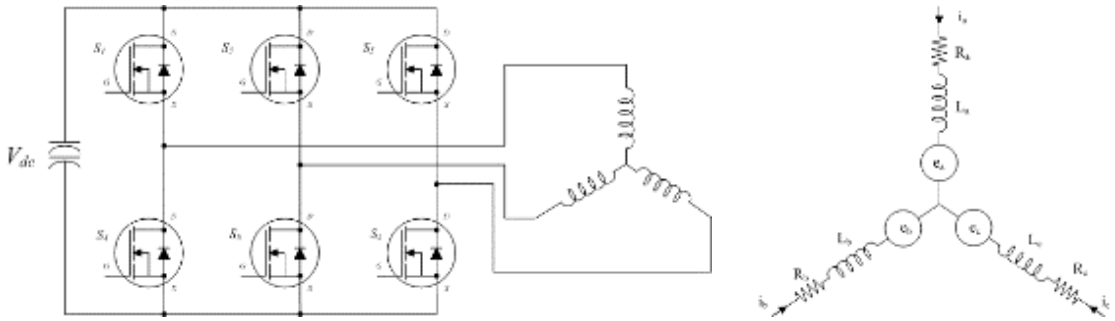

Figure 6. Inverter configuration and stator equivalent circuit

The BLDC motor can be represented as

$$v = Ri + \frac{d}{dt}\left[L_s(\theta_r)i + \lambda_M\right] = Ri + L_s(\theta_r)\frac{di}{dt} + i\omega_r \frac{d}{d\theta_r}L_s(\theta_r) + e. \quad (7)$$

However, the term of $i\omega_r dL(\theta_r)/d\theta_r$ is zero because there is no change in inductanc. Therefore, the motor can be represented as

$$\begin{aligned} v &= Ri + L_s\frac{d}{dt}i + e \\ \begin{bmatrix} V_a \\ V_b \\ V_c \end{bmatrix} &= \begin{bmatrix} R & 0 & 0 \\ 0 & R & 0 \\ 0 & 0 & R \end{bmatrix}\begin{bmatrix} i_a \\ i_b \\ i_c \end{bmatrix} + \begin{bmatrix} L_s & 0 & 0 \\ 0 & L_s & 0 \\ 0 & 0 & L_s \end{bmatrix}\frac{d}{dt}\begin{bmatrix} i_a \\ i_b \\ i_c \end{bmatrix} + \begin{bmatrix} e_{as} \\ e_{bs} \\ e_{cs} \end{bmatrix} \end{aligned} \quad (8)$$

where i_a, i_b, and i_c are phase currents, and V_a, V_b, and V_c are phase voltages, respectively. The electromagnetic torque is expressed as

$$T_e = \frac{1}{\omega_r}(e_{as}i_a + e_{bs}i_b + e_{cs}i_c). \quad (9)$$

where, J is inertia, T_L is load torque, and B is the viscous damping [8].

By considering the operation of the BLDC motor with six-switch inverter topology [1],[2], Figure 7 shows back-EMFs and phase currents, where the rotor is rotating in a counter clockwise (CCW) direction at a ω_m speed. This emf waveform has a flat portion, which occurs for at least 120° during each half-cycle. The amplitude E is proportional to the rotor speed. The back-emf constant is 2.35 mV/rpm, and maximum operating speed is 6,000 rpm. Therefore, the amplitude E is 14.1 V at 6,000 rpm. This point is important to design the motor and drive. The operating minimum input voltage should be larger than back-emf at the maximum speed.

Overall block-diagram of the BLDC motor drive is shown in Figure 8. The PWM electronics consists on the BLDC motor, motor drive and the magnetic encoder. In the BLDC motor, the switching logic of the motor drive is determined by rotor position. In order to detect the rotor position, hall sensors are used. The motor drive has been implemented on A3938 (Allegro). FDMC8030 (Fairchild) is used for the power switch. For precise position control, the position sensor is needed to be more accurate than hall sensors. For this reason, the magnetic encoder is applied. The magnetic encoder has been implemented on AS5050 (Austria Micro Systems) which has 10-bit resolution. Even if the integrated system is applied, the cost reduction is not significant. Because there are no difference of main electronics. However the volume of integrated system can be reduced significantly. Before integrating system, the length is approximately 70[mm]. But the integrated system is reduced to a length of 60[mm] because of a common case.

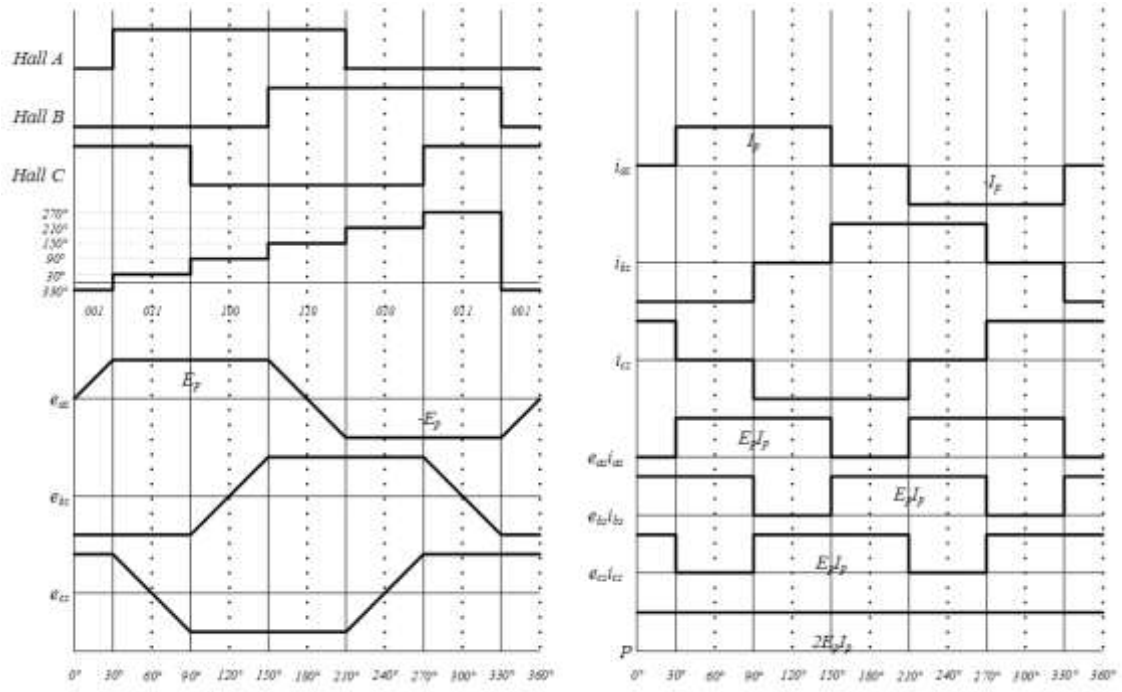

Figure 7. Waveforms of BLDC mtor

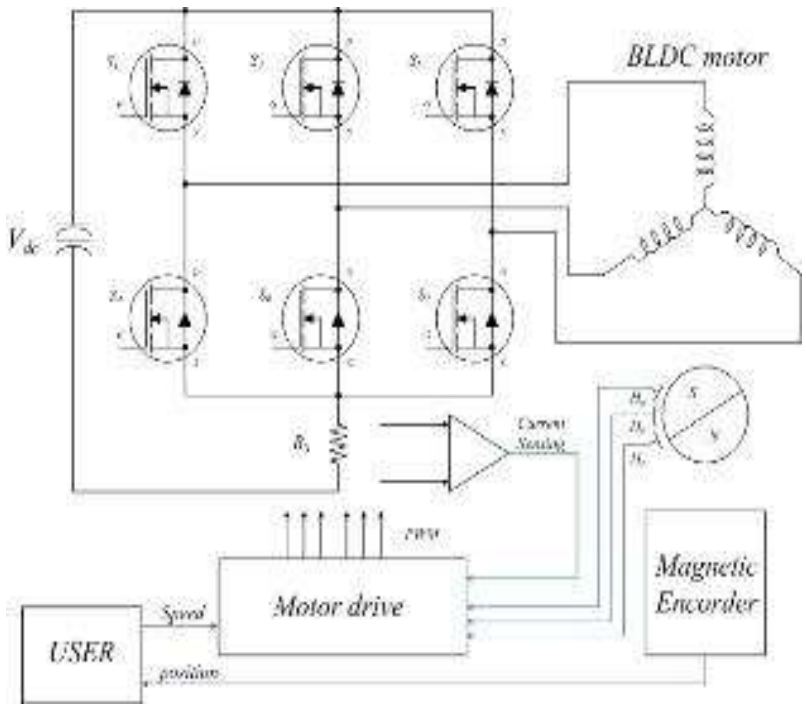

Figure 8. Overall block-diagram of BLDC motor drive

4. MEASURMENT AND VERIFICATION

Several experiments have been performed. Figure 9 shows final assembly of the motor and drive system and Figure 10 shows photos of the motor, the controller and the encoder. The drive and encoder were designed in the form of a round. The specifications of the drive and the encoder are shown in Table 2. Waveforms of output voltage and current are shown in Figure 11(a). The motor is operated well by hall sensor signal. Figure 11(b), (c), and (d) shows output waveforms which is changed by velocity of the motor.

Figure 9. Assembly of motor and drive system

Figure 10. Photos of motor, controller, and encorder

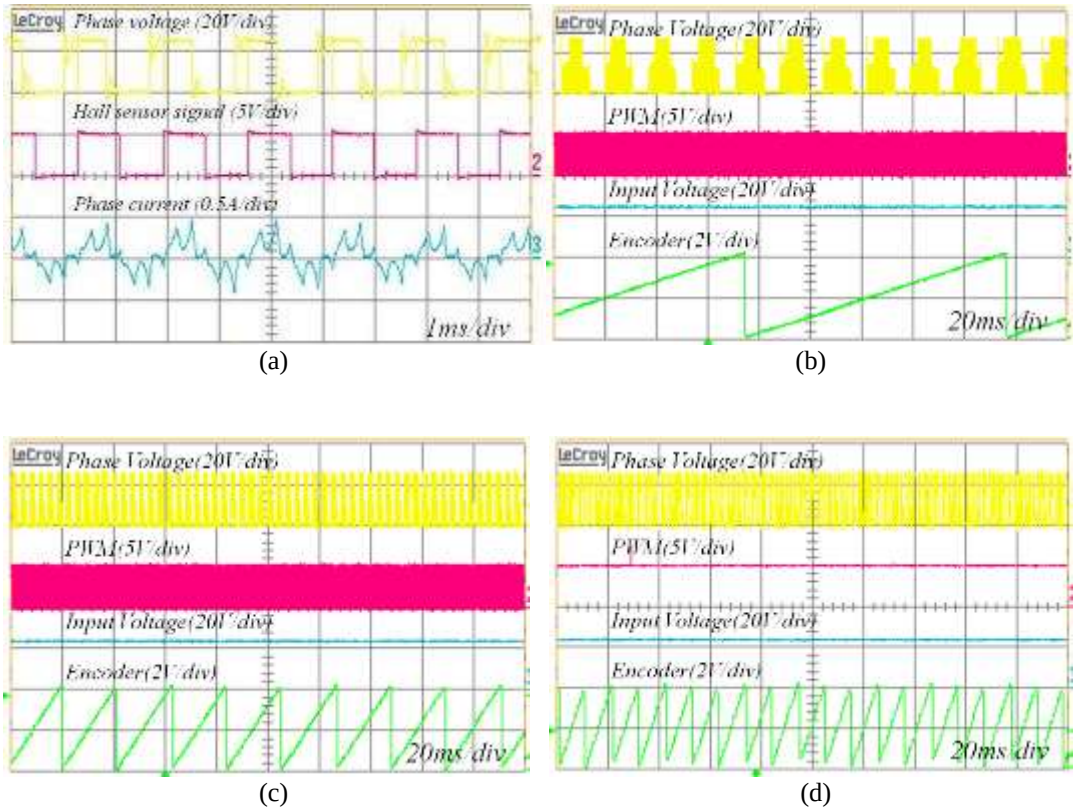

Figure 11. Waveforms of manufacture motor

Table 2. Specifications of drive and encorder

Item	Unit	Value
Maximum ouput	W	19.6
Maximum efficiency	%	63
Output density	W/g	0.12
Encoder resolution	ppr	4,096
Diameter of encoder	Mm	35
Diameter of drve	mm	35
Thickness of encoder	mm	11
Thickness of drive	mm	4

For the load test, the BLDC motor with integrated the inverter system is connected to torque measuring system as in Figure 12 (a). Measurement equipments consist of DC power supply to supply power, dynamometer for output characteristics, powermeter for measuring power, and computer for display and load control. Figure 12 (b) shows output characteristics of the BLDC motor. As shown in Figure 12 (b), no load speed is about 5,400[rpm] and maximum efficiency is 63 [%].

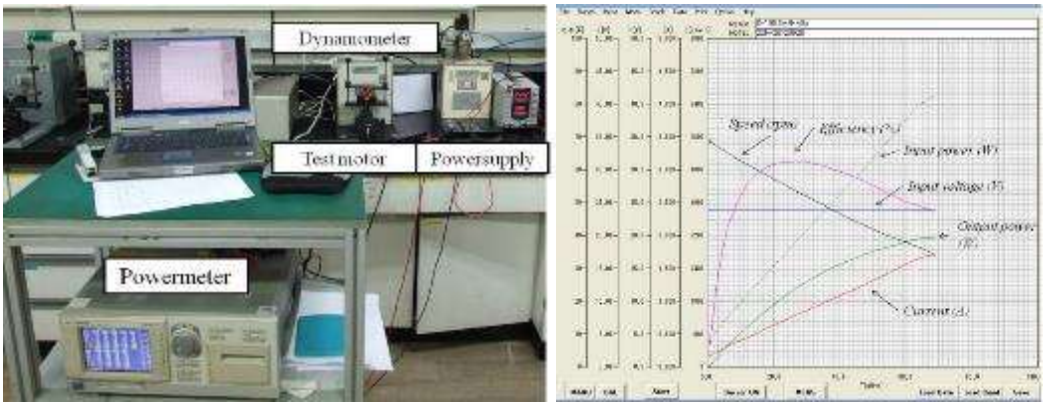

(a) Test setup (b) NTI curve

Figure 12. Test setup and results

5. CONCLUSION

This paper presents a design and implementation of integrated power electronics for industrial applications. It is important to consider integration. In order to integrate system, the BLDC motor, the drive, and the encoder module are designed considering the assembly. Through the experimental results, validity of the reported designs is verified, and the BLDC motor and drive are obtained the 63 % of maximum efficiency. The developed motor system can have been successfully applied the systems.

REFERENCES

[1] T. J. E. Miller, *et al.*, "Design of Brushless Permanent-Magnet Motors," Magna Physics publishing and Clarendon Press, Oxford, 1994.
[2] R. Valentine, "Motor Control Electronics Handbook," McGrow-Hill Handbook, 1998.
[3] G. R. Slemon, "High-efficiency drives using permanent-magnet motors," in *IEEE IECON conference*, pp. 725-730, 1993.
[4] V. R. Stefanovic, "Opportunities in motor drive research – a view from industry," in *IEEE IECON conference*, pp. 37-44, 1995.
[5] M. A. Rahman, "Modern electric motors in electronic world," in *IEEE IECON'93 conference*, pp. 644-648, 1993.
[6] J. M. Seo, *et al.*, "A study on brushless DC motor high torque density," *WASET*, vol. 58, pp. 225-229, 2011.
[7] D. Hanselman, "Brushless Permanent Magnet Motor Design," second edition, The writers' collective, 2003.
[8] R. Krishnan, "Electric Motor Drives: Modeling, Analysis, and Control," Prentice Hall, 2001.